metals

MDPI

Article

Use of Ion-Exchange Resins to Adsorb Scandium from Titanium Industry's Chloride Acidic Solution at Ambient Temperature

Eleni Mikeli [1,*], Danai Marinos [1], Aikaterini Toli [1], Anastasia Pilichou [1], Efthymios Balomenos [2] and Dimitrios Panias [1]

[1] Laboratory of Metallurgy, School of Mining and Metallurgical Engineering, National Technical University of Athens (NTUA), Heroon Polytechniou 9, 15780 Zografou, Greece; dmarinou@metal.ntua.gr (D.M.); katerinatoli@metal.ntua.gr (A.T.); anastasiapilichou@mail.ntua.gr (A.P.); panias@metal.ntua.gr (D.P.)

[2] Mytilineos S.A, Metallurgy Business, Agios Nikolaos, 32003 Voiotia, Greece; efthymios.balomenos-external@alhellas.gr

* Correspondence: elenamikeli@mail.ntua.gr; Tel.: +30-210-7722-177

Abstract: Scandium metal has generated a lot of interest during the past years. This is due to the various crucial applications it has found ground in and the lack of production in countries outside China and Russia. Apart from rare earth ores, scandium is present in a variety of wastes and by-products originating from metallurgical processes and is not currently being sufficiently valorised. One of these processes is the production of titanium dioxide, which leaves an acidic iron chloride solution with a considerably high concentration of scandium (10–140 ppm) and is currently sold as a by-product. This research aims to recover scandium without affecting the solution greatly so that it can still be resold as a by-product after the treatment. To achieve this, two commercial ion-exchange resins, VP OC 1026 and TP 260, are used in the column setup. Their breakthrough curves are plotted with mathematical modelling and compared. Results indicate that VP OC 1026 resin is the most promising for Sc extraction with a column capacity of 1.46 mg/mL, but Zr, Ti, and V coextract have high capacities, while Fe does not interfere with the adsorption.

Keywords: scandium; titanium dioxide industry; ion-exchange resins; VPOC1026; TP260; nonlinear regression

Citation: Mikeli, E.; Marinos, D.; Toli, A.; Pilichou, A.; Balomenos, E.; Panias, D. Use of Ion-Exchange Resins to Adsorb Scandium from Titanium Industry's Chloride Acidic Solution at Ambient Temperature. *Metals* **2022**, *12*, 864. https://doi.org/10.3390/met12050864

Academic Editor: Antonije Onjia

Received: 31 March 2022
Accepted: 13 May 2022
Published: 18 May 2022

1. Introduction

Scandium (Sc) is the most valuable element among the rare earth elements (REEs) because of its application in many cutting-edge technologies such as metal halide lamps, high strength Al-Sc alloys (aerospace industry, baseball bats, military and medical purposes, and bicycle frames), scandia-stabilised zirconia as a high-efficiency electrolyte in solid oxide fuel cells, and as a tracer in cruel-oil refinery [1–3]. In the most recent report by the EU, Scandium is considered a Critical Raw Material (CRM) because of its high supply risk and economic importance [4]. The production of Sc has been modest to date (~16.3 t/y for 2018), while the demand for this metal is expected to gain a significant increase (up to 300 t/y) by 2028 [5]. At the same time, the Sc supply in Europe depends solely on imports, mainly from China (66%), Russia (28%), and Ukraine (7%) [4]. The abundance of scandium in the earth's crust is comparatively high (20–30 ppm), but it is sparsely dispersed and found in trace amounts in a variety of ores such as ilmenite, rutile, bauxite, nickel-laterite, tungsten, tin, and uranium [1,6–9]. During the industrial processing of these ores, Sc is usually accumulated in the waste streams (solid, liquid, or gas). Many researchers have studied the potential use of these wastes to recover Sc [3,10].

A large amount of the Sc_2O_3 produced in China originates from the titanium oxide (TiO_2) pigments production industries [6,11]. Other countries, such as European ones, which are currently solely dependent on imports of Sc, can benefit from the TiO_2 pigment industries to produce Sc as a by-product. Both in the sulfuric and chloride process of

TiO_2 production, most of the Sc ends up in the iron-rich residual solution (10–140 ppm of Sc) [1,6,8,12,13] together with other CRMs such as vanadium (V) and niobium (Nb) [13]. The ferrous chloride solution is usually sold to chemical industries and used as a coagulation/flocculation agent and for odour control, or its neutralised filter cake is landfilled without valorising the present CRMs.

Purification of scandium-containing streams is a challenging task. Unwanted elements, defined as impurities, are typically present in more than 10 times higher concentrations. Precipitation, which is the traditional approach for metal liquor purification, is prohibited as a stand-alone method for scandium extraction since metal impurities often coprecipitate, resulting in poor Sc purity [14,15]. In general, solvent extraction (SX) is the most employed separation/purification technique for recovering Sc, as it shows high extraction capacities and is easily scalable. The Sc that is recovered from the titanium acidic side streams is also separated with SX. The most common extraction systems that have been examined by many researchers and are currently applied in China's scandium extraction plants are a mixture of D2EHPA and TBP [1,6,8,9,12,16] Despite the benefits, the SX also possesses some drawbacks, the most important one being the losses of the organic extractants which usually contaminate the solution as well [17,18].

Among the technologies for the separation and purification of aqueous solutions, ion exchange (IX) has some benefits compared with SX techniques: less contamination of the pregnant solution, lower operation costs [18], etc., and thus, it has attracted a lot of attention for scandium extraction [7,15,17–27]. The stable oxidation state of scandium in an aqueous solution is Sc(III) [28]. Scandium-hydrated ions are Pearson hard acids because of their high oxidation state, and they choose to form complexes with hard ligands, including hydroxide, fluoride, sulfate, and phosphate [28]. According to Wang et al. [14], organophosphorus compounds such as phosphoric, phosphonic, and phosphinic acid, as well as neutral phosphine oxides, have been effective in the quantitative extraction of scandium from aqueous solution through solvating and the cation-exchange mechanisms.

Along with the wide variety of commercial and custom-made resins that have been used, Lewatit VP OC 1026 and Lewatit TP 260 seem promising [18,21–23,29] for the selective extraction of Sc. Mostajeran et al. [23] studied the use of VP OC 1026 in a sulfuric acid pregnant leaching solution (PLS), which resulted from coal fly ash leaching and reported fast adsorption kinetics for Sc and high selectivity for Sc towards Fe and Al. Reynier et al. [29] conducted bioleaching of uranium tailings and utilised a variety of IX resins. Among them, VP OC 1026 and TP 260 showed high extraction of Sc but with high coextraction of U and Th and low coextraction of Fe. In another study [18], the TP 260 IX resin was used to extract REEs from phosphoric acid solutions; the results showed very high recovery rates for Sc (80%) and reported the ions of Al and Fe to be the most interfering in terms of coextraction. Bao et al. [22] studied the recovery of Sc from sulfuric acid solutions using IX resins and reported a slow adsorption rate for TP 260. In addition, they showed that the selectivity order for TP 260 resin is Sc(III) > Fe(III) > Al(III) > Fe(II). Rychkov et al. [21] conducted kinetic experiments with TP 260 in sulfuric acid solutions and showed that Th, Fe, and Al are sorbed in the intradiffusion mode while Sc, Ti, and Zr are sorbed in the mixed diffusion mode.

This paper examines the potential utilisation of a by-product of the TiO_2 industry for Sc extraction through the ion-exchange purification technique. More particularly, a real solution derived from a European TiO_2 industry was loaded directly into the column setup, imitating an actual ion-exchange process. Two different commercial resins are examined and compared using a fixed-bed column setup: Lewatit VP OC 1026, a bis(2-ethylhexyl)phosphoric acid (D2EHPA) in a cross-linked polystyrene matrix and Lewatit TP 260, a macroporous cross-linked polystyrene with an aminomethyl-phosphonic acid functional group.

The evaluation of such experiments can be challenging, from data analysis to experimental and analytical point of view, as the feed solution is a multicomponent industrial-grade solution, but also the column setup is a dynamic procedure. For this reason, triplicate

experiments were conducted, and mathematical modelling was applied for the data analysis. Assessing the ion-exchange procedure was focused not only on the loading behaviour of Sc but also on its selectivity towards Zr, Ti, V, and Fe because the literature showed that these metals might impede Sc extraction. Even though the combined effect of these metals has not been studied using these two resins, studies in similar extraction systems indicate that Sc extraction is influenced when these metal impurities are present since they exhibit similar chemical behaviour and extraction rates [21,26,30].

2. Materials and Methods

2.1. Materials and Experimental Procedure

Two different commercial resins were used in this study provided by Lenntech (Delfgauw, The Netherlands). In Table 1, the main characteristics of the resins are listed, and in Figure 1, the functional groups of each resin are illustrated. Before the column experiments, an adequate quantity of Lewatit TP 260 resin was conditioned in three cycles with 1.5 M HCl solution, in a ratio of 1/10 for 2 h to be converted into the hydrogen form, according to the available datasheets. Lewatit VP OC 1026 resin was received in hydrogen form; hence, no conditioning step was required.

Table 1. Resins characteristics.

Resin Name	Lewatit VP OC 1026	Lewatit TP 260
Functional group	bis(2-ethylhexyl)phosphoric acid (D2EHPA)	aminomethyl-phosphonic acid (AMPA)
Matrix	Cross-linked polystyrene	Cross-linked polystyrene
As received form	H^+	Na^+
Bead size range	0.3–1.6 mm	0.4–1.25 mm

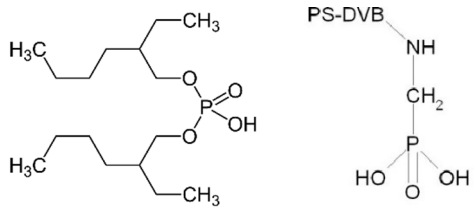

(**a**) (**b**)

Figure 1. Functional groups of the two commercial resins (**a**) Lewatit VP OC 1026 and (**b**) Lewatit TP 260.

The feed solution used in this study is an acidic $FeCl_2$ solution that originated from the titanium dioxide pigment industry of Europe. The chemical analysis of the main elements of the solution is illustrated in Table 2.

Table 2. Chemical analysis of $FeCl_2$ feed solution.

Metals	Fe (II)	Fe (III)	Mn	Al	Mg	Na	V	Zr	Ca	Cr	Ti	Sc
Concentration (g/l)	110.5	1.5	19.09	9.11	8.34	6.41	4.20	3.68	2.36	1.69	0.528	0.130

For the fixed-bed column experiments, laboratory borosilicate glass columns with 20 mL bed volume, 1.5 cm × 10 cm dimensions were used. The top and bottom of the column had fixed caps with a luer lock inlet and outlet fittings for tubing attachment. A known weight of the resin was packed into the column. The $FeCl_2$ solution continuously passed through the column in an upward constant flow of 0.93 BVh^{-1}, with the use of a peristaltic pump LabDos, from Hitec Zang. Samples of the effluent solution were fractionally collected from the top of the column to perform a chemical analysis of the metals of interest (Fe, Ti, Sc, V, and Zr).

Wet chemical analysis of the samples was carried out using the inductively coupled plasma–optical emission spectrometry (ICP-OES), Optima 8000 by Perlin Elmer (Waltham, MA, USA). Calibration standard solutions were prepared from commercially available ICP, Ti, Sc, V, Zr, and Fe standards (1000 ppm) obtained from Merck (Darmstadt, Germany). The standard solutions were prepared in a suitable concentration and diluted further with 1% *v/v* analytical grade nitric acid (65% wt.) as required for working standards. High purity deionized water (18.2 MΩ/cm) and argon of special purity (99.999%) were used. Re was used as the Internal Standard (IS) for samples and standards in the case of V and Zr analysis in order to correct the signal drift and reduce the interferences from Fe.

2.2. Mathematical Modelling

2.2.1. Mathematical Description of the Fixed-Bed Columns

The total capacity of the column can be calculated for every metal of interest, q_{Me} (mg M_e per mL of resin), by integrating the plot of the adsorbed metal concentration C_{ad} (mg/L) against the effluent volume, V_{Ef} (mL) [31]. The area, A, under this integrated plot is substituted in Equation (1):

$$q_{Me} = \frac{A}{1000V_{resin}} = \frac{\int_{V_i=0}^{V_i=total} C_{ad}dV_i}{1000V_{resin}} \quad (1)$$

where C_{ad} is the difference between the initial concentration and the instant concentration of the effluent solution ($C_{ad} = C_0 - C_i$), and V_{resin} is the volume of resin packed into the column (mL).

The total removal efficiency (E%) of each metal can be calculated from Equation (2):

$$E\% = 100\frac{m_{total,ads}}{m_{total,in}} \quad (2)$$

where $m_{total,ads}$ is the cumulative amount of metal adsorbed in the resin, and $m_{total,in}$ is the cumulative amount of metal entering the resin.

2.2.2. Modelling of Experimental Results through Regression Method

The performance of fixed-bed column adsorption is typically evaluated through the plot of the dimensionless concentration of the effluent solution versus the eluted volume or time [32–35]. This plot is referred to as the breakthrough curve. In the literature, many models have been developed to describe the breakthrough curve of a fixed-bed column, either based on empirical relationships or based on different assumptions regarding the kinetics and mechanism of extraction. In our study, the Thomas model was chosen as the most extensively reported mathematical model for predicting breakthrough curves [36]. This model was developed from the equation of mass conservation in a flow system assuming plug flow, equilibrium described by Langmuir isotherm, and second-order reversible kinetics. Particularly, it neglects internal and external diffusion effects [32]. The equation for the Thomas model is demonstrated in Equation (3):

$$\frac{C_i}{C_0} = \frac{1}{1 + \exp\left[\left(\frac{K_{Th}}{Q}\right)\left(q_{Th}V_{resin} - \frac{C_0V_i}{1000}\right)\right]} \quad (3)$$

where Q is the volumetric flow rate (mL/min), V_{resin} is the volume of resin packed into the column (mL), and C_0 and C_i represent the initial concentration of the feed solution and the effluent concentration (mg/L), respectively, V_i is the effluent volume (mL), K_{Th} (mL/min g) is the Thomas rate constant, and q_{Th} (mg/mL) represents the adsorption capacity of the fixed beds.

Linear regression is the most typical method for fitting experimental results [31,37,38], where the calculation of the model parameters becomes associated with the slope and

intercept of a straight line. The linearised form of the Thomas model is illustrated in Equation (4):

$$\ln\left(\frac{C_0}{C_i} - 1\right) = \frac{K_{Th} q_{Th} V_{resin}}{Q} - \frac{K_{Th}}{Q1000} C_0 V_i \quad (4)$$

It is evident that the error distortion created by linearisation may lead to misleading results [39]. The linear transformation strongly modifies error distribution and alters the weight associated with each point, either for the worse or for the better [40]. An alternative to linear regression is nonlinear regression. In this method, model parameters are first estimated and, through a trial and error procedure, evolve towards the values that minimise a given error function, i.e., the sum of squares error (SSE) Equation (5), based on a selected algorithm.

With the advancement of computing technology, nonlinear least-squares regression is now easier to implement with common mathematical tools such as Microsoft Excel's Solver. Moreover, nonlinear regression has been shown to be more stable and less susceptible to experimental error [32,34]:

$$SSE = \sum_{i=1}^{n} (y_c - y_e)_i^2 \quad (5)$$

where n is the number of experimental data points, y_c is the predicted (calculated) data with the Thomas model, and y_e is the experimental data.

3. Results and Discussion

3.1. Breakthrough Curve Data Fitting

Normally, fixed-bed column adsorption is a dynamic procedure where both the kinetics of the reaction as well as the mass balance are constantly changing [41]. The analysis of such experiments can be challenging as both these factors should be considered. A valid method for evaluating such studies that have been utilised in the literature is through mathematical modelling [31,34,41–43]. In this work, Thomas's model was chosen for data fitting through nonlinear regression analysis.

In Table 3, the results from data fitting of the fixed-bed column loading experiments using the $FeCl_2$ solution for the two different resins are illustrated. The high R^2 values obtained from all curved through nonlinear regression indicate a good fit of the Thomas model to experimental data. Only in the case of V with the VP OC 1026 resin the correlation coefficient is lower than 0.95, showing a slight deviation from the Thomas model's theoretical assumptions. The plotted breakthrough curves, as well as the extraction curves for Sc, Ti, Zr, and V, are depicted in Figures 2 and 3 for VP OC 1026 and TP 260 resins, accordingly.

Table 3. The results of nonlinear regression analysis with Thomas mathematical model for VP OC 1026 and TP 260 resin.

Resin	Metal	R^2	K_{Th} (mL/min g)	q_{Th} (mg/mL)
VP OC 1026	Sc	0.981	0.069	1.46
	Ti	0.965	0.036	2.2
	Zr	0.959	0.005	15.9
	V	0.887	0.009	4.06
TP 260	Sc	0.991	0.310	0.46
	Ti	0.978	0.043	1.98
	Zr	0.988	0.013	8.7
	V	0.973	0.039	4.86

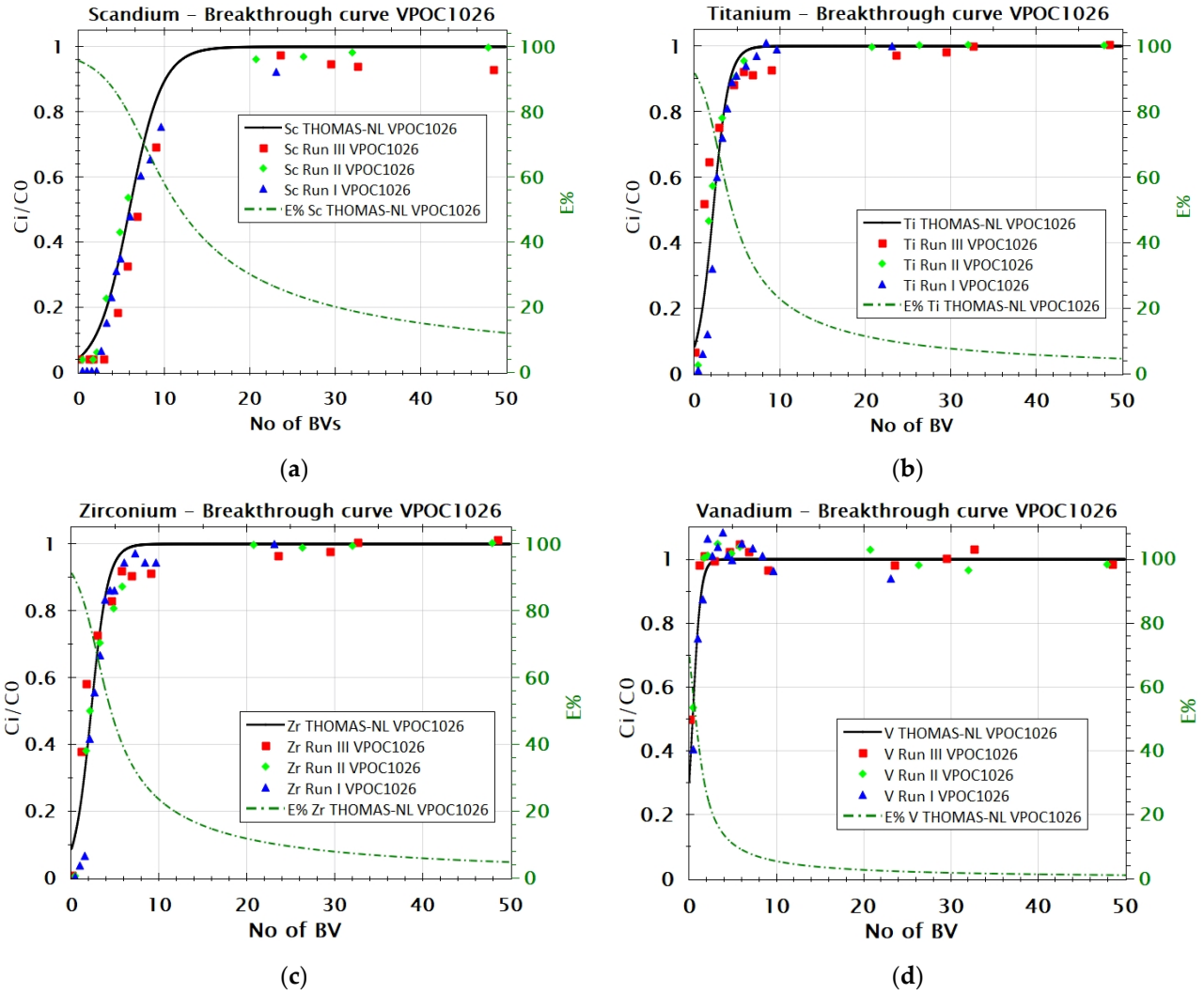

Figure 2. Extraction and breakthrough curves for VP OC 1026 resin for (**a**) Sc, (**b**) Ti, (**c**) Zr, and (**d**) V were measured in three different experimental runs and their Thomas nonlinear (NL) prediction mathematical model.

For the VP OC 1026 resin, the time to reach exhaustion ($C_i/C_0 = 0.9$) for Sc is estimated at 10BV for Zr and Ti 4.3BV, and 1BV for V according to Thomas nonlinear model (Figure 2). When the volume of effluent does not exceed 5.8 BV, the extraction of Sc from the $FeCl_2$ solution using VPOC1026 resin is greater than 80%, while the coextraction of other metals is at 9.5% for V, 39% for Ti and 40% for Zr.

According to the Thomas nonlinear model for TP 260 resin, the time to attain exhaustion (Ci/C0 = 0.9) for Sc is estimated at 3BV and 2BV for Zr, 4BV for Ti, and 1BV for V (Figure 3). Sc extraction from $FeCl_2$ solution using this resin is higher than 80% when the effluent volume is less than 2.6 BV, while the coextraction of other metals is 77% for Ti, 56.5% for Zr, and 27.5% for V.

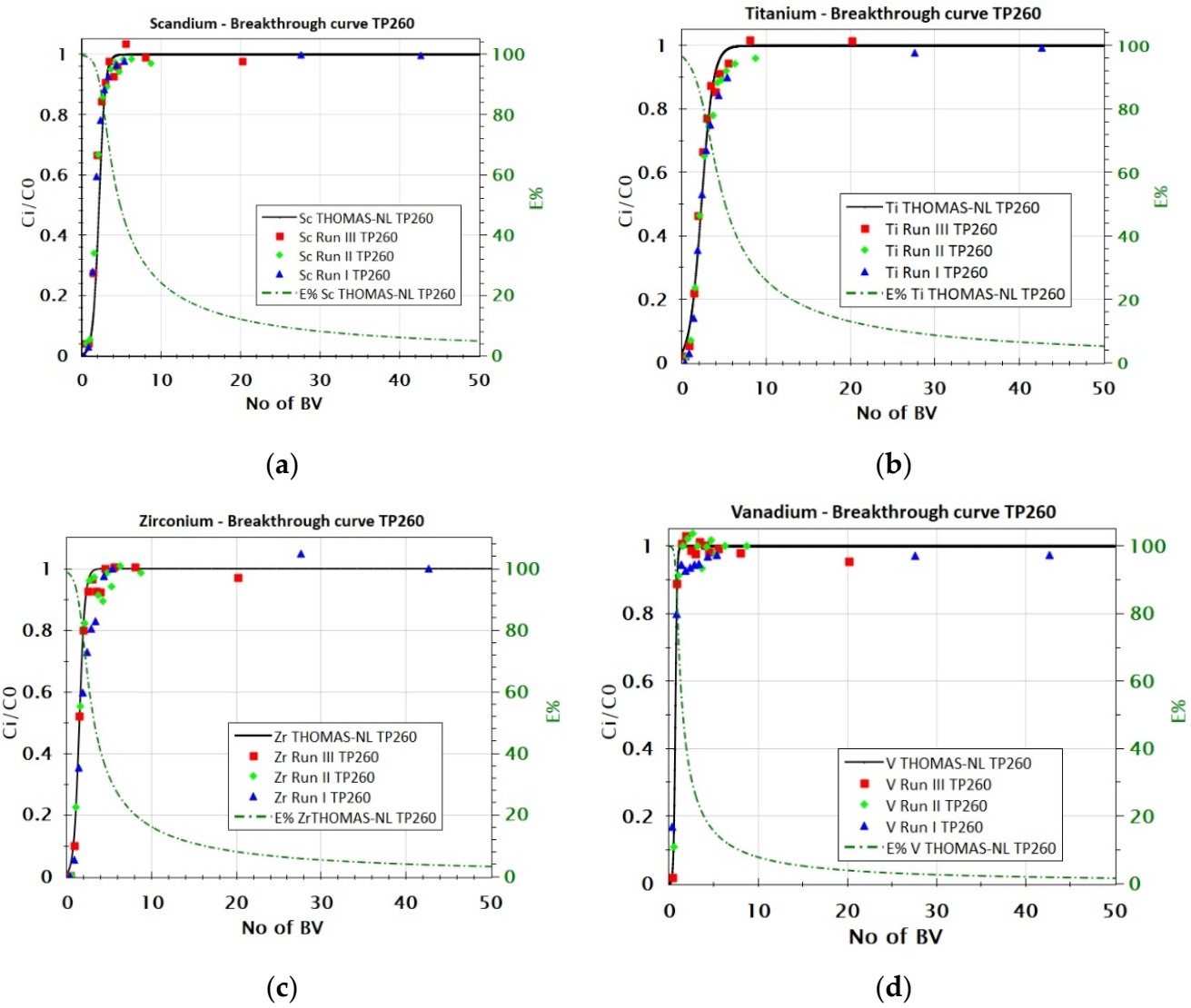

Figure 3. Extraction and breakthrough curves for TP 260 resin for (**a**) Sc, (**b**) Ti, (**c**) Zr, and (**d**) V were measured in three different experimental runs and their Thomas nonlinear (NL) prediction mathematical model.

3.2. Resins Adsorption Behavior

3.2.1. Adsorption Behavior of Sc, Ti, Zr, and V from $FeCl_2$ Solution with VP OC 1026 Resin

In Figure 4, the breakthrough curves for VP OC 1026 are compared for all the metals of interest. For V, the curve is steeper, and the breakpoint appears early, indicating a fast uptake making it the weakest adsorbed component. The curve plot is almost identical for Zr and Ti. Even though there are no references available on the adsorption of Zr and Ti on VP OC 1026 resin, it is reported that these metals interfere with Sc extraction in solvent extraction systems with D2EHPA, which is also the resin's functional group [26]. Sc breakpoint and saturation appear later than the other metals, showing that Sc is a strongly adsorbed component, confirming the high affinity of Sc with D2EHPA reported in other studies [44].

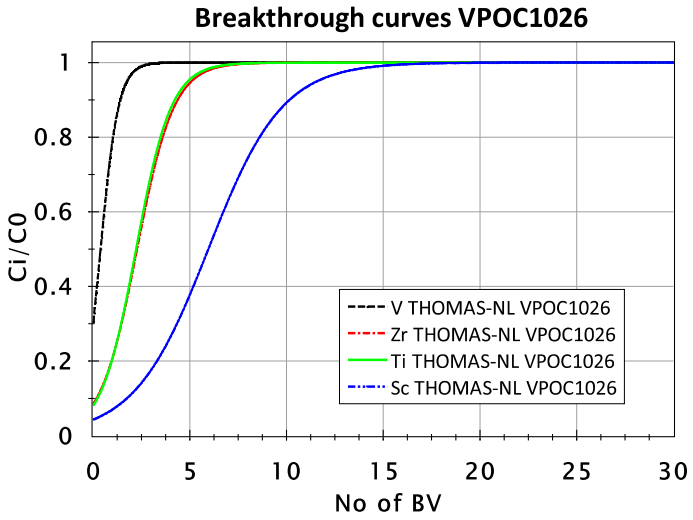

Figure 4. The comparative breakthrough curve for the metals of interest for VP OC 1026 resin according to Thomas nonlinear (NL) prediction mathematical model.

3.2.2. Adsorption Behavior of Sc, Ti, Zr, and V from $FeCl_2$ Solution with TP 260 Resin

TP 260 resin adsorbs the metals at a similar rate without showing any selectivity towards any metal (Figure 5). This observation is confirmed by the kinetic study of Rychkov et al. in sulfuric acid solutions using TP 260 resin, where it was observed that Zr, Ti, and Sc are adsorbed by the resin following the same kinetic model [21].

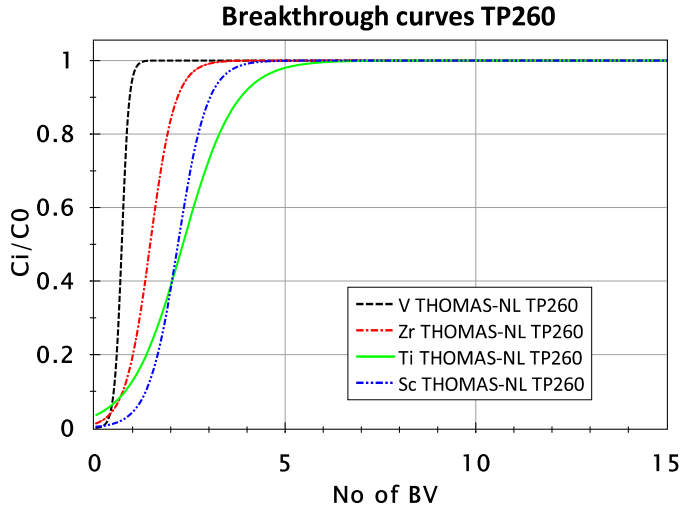

Figure 5. The comparative breakthrough curve for the metals of interest for TP 260 resin according to Thomas nonlinear (NL) prediction mathematical model.

3.2.3. Adsorption Behavior of Fe with VP OC 1026 and TP 260 Resins

In this section, the results regarding the adsorption behaviour of Fe are illustrated for both VP OC 1026 and TP 260 resin. The experimental breakthrough curves of Fe for both resins can be seen in Figure 6.

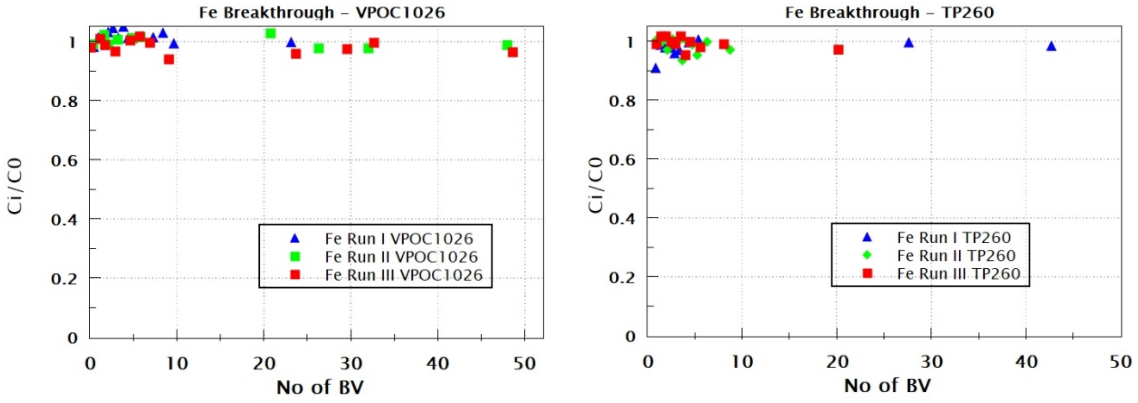

(**a**) (**b**)

Figure 6. Chemical analysis results of Fe for VP OC 1026 (**a**) and TP 260 (**b**) resin throughout adsorption experiments.

Despite the high content of Fe in the feed solution, the results presented in Figure 6 show that no significant adsorption profile can be identified. This behaviour provides a huge advantage for the potential utilization of the examined resins, as the resins can operate by leaving the Fe content in the solution unchanged and separating it from Sc. The above observation is not in line with the research of Heres et al. [18], where iron was always coextracted with REEs from phosphate media, and it significantly reduced the loading of REEs, including Sc. This is probably due to either the different matrix of the solution examined (phosphoric media vs. chloride media) or the presence of trivalent Fe in these solutions. According to the study by Bao et al. [22], Fe(III) coextracts with Sc in cation solvent extraction and ion exchange, most likely because iron (III) competes more strongly with Sc than Fe(II) because of its similar charge density and size (II).

3.2.4. Comparison of VP OC 1026 and TP 260 Resins' Loading Capacity

The column capacity q (mg/mL), as a function of the effluent volume, can be integrated through the combination of Equations (1) and (3). The diagrams in Figure 6 compare the two resins for each metal to demonstrate the loading of the column as a function of the volume of effluent solution, expressed in bed volume (BV).

Mostajeran et al. [23] studied the adsorption behaviour of VP OC 1026 resin from synthetic sulfuric acid solution and defined 8 mg Sc/mL resin loading from a feed solution with 100–150 ppm of Sc. According to Mostajeran et al., this value is the maximum capacity of the resin in such a solution as a 1:1 molar ratio reaction between Sc and solvent molecules was confirmed. In our study, the highest Sc column capacity achieved with VP OC 1026 resin from a feed solution with 130 ppm Sc estimated 1.46 mg/mL resin (Figure 7.), less than what was expected from the cited reference. This reduced loading can be mainly justified by the high coextraction of the other metals that are present in the $FeCl_2$ solution.

In our study, TP 260 has a maximum Sc loading capacity of 0.31 mg/mL resin (Figure 7). The performance of TP 260 resin is much lower than what was expected from other studies. Bao et al. [22] determined that the loading of TP 260 resin is 30 mg Sc/mL resin at pH 2.5 and 16 mg Sc/mL at pH 1 from a pure synthetic sulfuric acid solution, confirming the adsorption dependence on pH [33]. Antisel et al. [7] determined the loading capacity of TP 260 6 mg Sc/mL resin from a polymetallic sulfuric pregnant leach solution containing Al, Co, Fe, Mn, and Ni at a pH of 3.5. These findings suggest that the adsorption capacity of the resin is decreased substantially when other metals coexist in the feed solution. The comparatively low performance of TP 260 resin for Sc adsorption, reported in our work, can be attributed to the high acidity of the feed solution but also to the presence of the other metals Ti, Zr, and V that are coloaded in the resin.

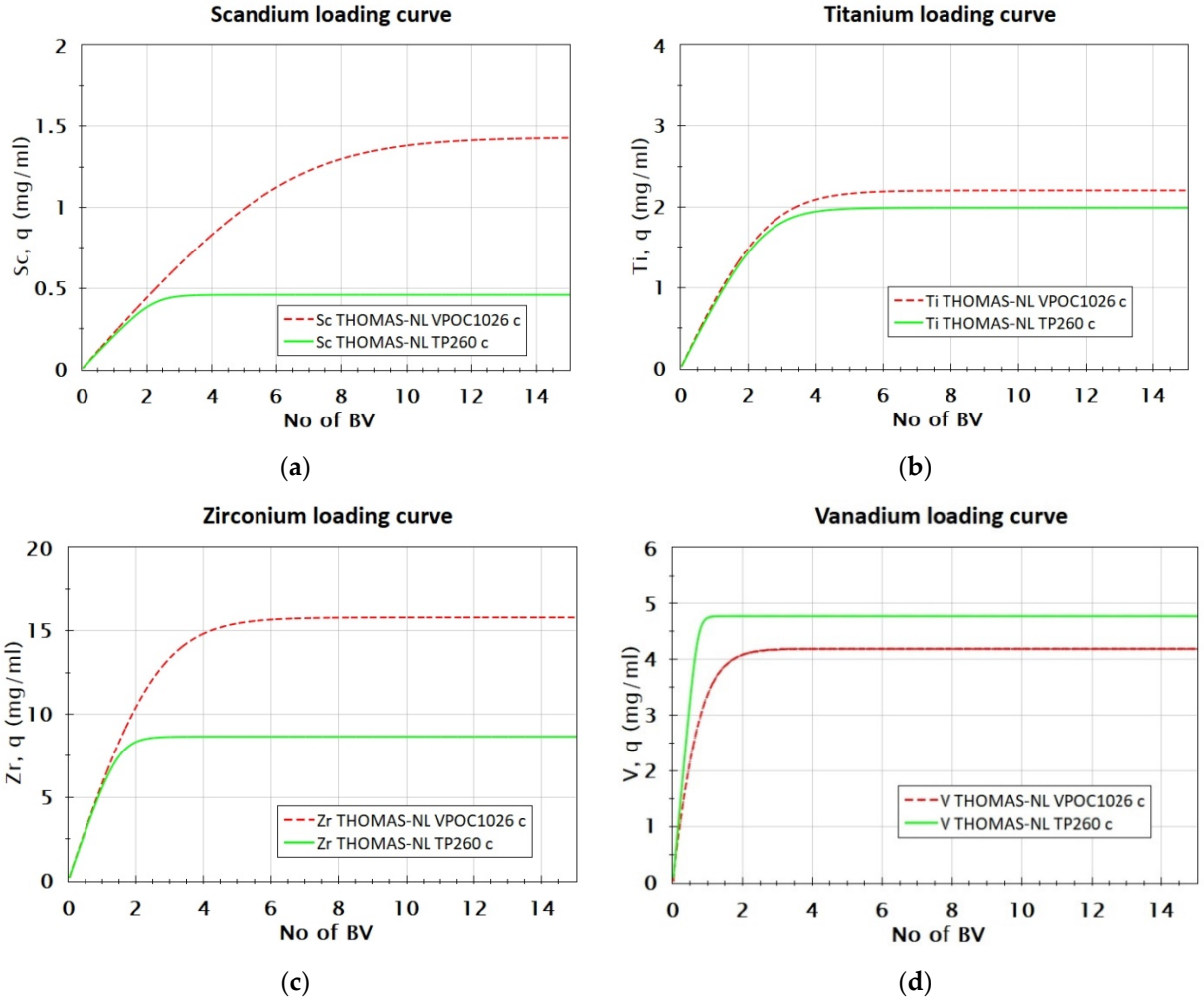

Figure 7. Breakthrough curve of (**a**) Sc, (**b**) Ti, (**c**) Zr, and (**d**) V for VP OC 1026 and TP 260 resin according to Thomas nonlinear (NL) prediction mathematical model.

Table 4 shows the ratio of metal concentration in VP OC 1026 resin to concentration in TP 260 resin.

Table 4. Ratios of metal's capacity in VP OC 1026 resin to TP 260 resin.

Metal, Me	$Me_{VPOC1026}/Me_{TP260}$
Sc	3.16
Zr	1.83
Ti	1.11
V	0.84

In VP OC 1026 resin, Sc loading (1.46 mg/mL resin) is more than three times higher, and Zr loading (15.9 mg/mL resin) is almost two times higher compared with TP 260 resin which is 0.46 mg/mL resin and 8.7 mg/mL resin, accordingly. The Ti loading is similar for both resins, 2 mg/mL resin, while V loading is slightly higher in TP 260 4.86 mg/mL resin compared with VP OC 1026 resin 4.06 mg/mL resin.

The mass ratios of Ti, Zr and V to Sc (Me/Sc) for the initial $FeCl_2$ solution and the two loaded resins are shown in Table 5. The ratio's lower values suggest a higher concentration of scandium.

Table 5. Ratios of metal impurities concentration to Sc concentration in the three examined phases: $FeCl_2$ solution, VP OC 1026 resin and TP 260 resin.

Ratio, Me/Sc	$FeCl_2$	VP OC 1026	TP 260
Zr/Sc	27.69	10.91	18.89
Ti/Sc	4.06	1.51	4.30
V/Sc	32.31	2.79	10.59

As shown in Table 5, the Me/Sc ratio is greater than 1 in every case, indicating metal impurities are always in excess. However, VP OC 1026 exhibits high selectivity for Sc extraction towards Zr, Ti, and V. The ratio Zr/Sc decreases from 27.69 in the initial feed solution to 10.91 in VP OC 1026 resin and for Ti is reduced from 4.06 to 1.51. Moreover, in VP OC 1026, the ratio of V/Sc is significantly reduced from 32.31 to 2.79. This suggests that the resin has a decreased affinity for V, despite its relatively high loading concentration in the resin (4.06 mg V/mL resin), which might be due to the high concentration of this metal in the feed solution.

The Ti/Sc ratio for TP 260 resin is raised to 4.3, compared to 4.06 in the original feed solution, showing that TP 260 resin has a larger affinity for Ti extraction towards Sc. All the metal ratios towards Sc are higher with TP 260 resin compared with the VP OC 1026, meaning that the latter is overall more selective for Sc in the given feed solution.

4. Conclusions

In this study, the Sc extraction through ion exchange technique was examined. The feed solution was an acidic $FeCl_2$ solution obtained from the TiO_2 industry. Two different commercial resins, VP OC 1026 and TP 260, were examined and compared under a standard loading experiment in a fixed-bed column setup. The capacity, the breakthrough, and the exhaustion of the column for Sc, but also for the basic metal impurities Zr, Ti and V were determined through mathematical modelling of the column. The Thomas model provided a very good fit to the experimental data, with R^2 higher than 0.98 for Sc, higher than 0.95 for Zr and Ti and higher than 0.88 for V.

For both resins, the Fe adsorption is insignificant, suggesting that the resins could be utilised for separating Sc from the solution without affecting the initial Fe content of the feed solution, which was an important objective of this study. The results indicate that VP OC 1026 is the most promising resin for scandium extraction, showing a higher capacity of Sc 1.46mg/mL in the given experimental conditions. The metals Zr, V, and T present in the initial solution are also coextracted in both resins' tests. It is important to note that the performance of the resins for Sc extraction should not be assessed merely based on the column's capacity. Even though Zr, V, and Ti have higher capacity values in the loaded resins, especially in VP OC 1026, the upgrade in Sc concentration is higher than the other metals. This indicates a high affinity of VP OC 1026 for Sc, while TP 260 resin shows a higher affinity for Ti.

Author Contributions: Conceptualization, E.M., D.M, A.T. and D.P.; methodology, E.M., A.T. and D.M.; validation, D.M, A.T. and A.P.; data curation E.M. and A.P.; writing—original draft preparation, E.M., D.M. and A.P.; writing—review and editing, E.B. and D.P.; supervision E.B. and D.P.; All authors have read and agreed to the published version of the manuscript.

Funding: This research was funded by EIT-KIC, ScaVanger Project (2021–2024), project number 20093.

Data Availability Statement: The data presented in this study are available on request from the corresponding author.

Acknowledgments: The resins used in this paper were provided by MEAB, Germany.

Conflicts of Interest: The authors declare no conflict of interest.

References

1. Shibata, J.; Murayama, N. Solvent Extraction of Scandium from the Waste Solution of TiO_2 Production Process. *Trans. Indian Inst. Met.* **2016**, *70*, 471–477. [CrossRef]
2. Hartley, C.J.; Hazen, W.W.; Baughman, D.R.; Bemelmans, C.M.A.; Belits, P.F.; Lanyk, T.J.; Porter, B.F.; Liao, L.; McAllister, J.; Yang, M.S.-Y. Methods of Recovering Scandium from Titanium Residue Streams. U.S. Patent No. 9,102,999, 11 August 2015.
3. Botelho Junior, A.B.; Espinosa, D.C.R.; Vaughan, J.; Tenório, J.A.S. Recovery of scandium from various sources: A critical review of the state of the art and future prospects. *Miner. Eng.* **2021**, *172*, 107148. [CrossRef]
4. European Commision. *Critical Raw Materials Resilience: Charting a Path towards greater Security and Sustainability*; European Commision: Brussels, Belgium, 2020.
5. Petrakova, O.; Kozyrev, A.; Suss, A.; Panov, A.; Gorbachev, S.; Perestoronina, M.; Vishnyakov, S. BR04-Industrial Trials Results of Scandium Oxide Recovery from Red Mud at UC RUSAL Alumina Refineries. *Ser. Geol. Tech. Sci.* **2020**, *4*, 156–165.
6. Zhang, L.; Zhang, T.-A.; Lv, G.; Zhang, W.; Li, T.; Cao, X. Separation and Extraction of Scandium from Titanium Dioxide Waste Acid. *JOM* **2021**, *73*, 1301–1309. [CrossRef]
7. Altinsel, Y.; Topkaya, Y.; Kaya, Ş.; Şentürk, B. *Extraction of Scandium from Lateritic Nickel-Cobalt Ore Leach Solution by Ion Exchange: A Special Study and Literature Review on Previous Works*; Springer: Cham, Switzerland, 2018; pp. 1545–1553. [CrossRef]
8. Li, Y.; Li, Q.; Zhang, G.; Zeng, L.; Cao, Z.; Guan, W.; Wang, L. Separation and recovery of scandium and titanium from spent sulfuric acid solution from the titanium dioxide production process. *Hydrometallurgy* **2018**, *178*, 1–6. [CrossRef]
9. Chen, Y.; Ma, S.; Ning, S.; Zhong, Y.; Wang, X.; Fujita, T.; Wei, Y. Highly efficient recovery and purification of scandium from the waste sulfuric acid solution from titanium dioxide production by solvent extraction. *J. Environ. Chem. Eng.* **2021**, *9*, 106226. [CrossRef]
10. Chernoburova, O.; Changes, A. The Future of Scandium Recovery from Wastes. In Proceedings of the International Conference on Raw Materials and Circular Economy, Athens, Greece, 5–9 September 2021.
11. Zhou, J.; Ning, S.; Meng, J.; Zhang, S.; Zhang, W.; Wang, S.; Chen, Y.; Wang, X.; Wei, Y. Purification of scandium from concentrate generated from titanium pigments production waste. *J. Rare Earths* **2020**, *39*, 194–200. [CrossRef]
12. Qiu, H.; Wang, M.; Xie, Y.; Jianfeng, S.; Huang, T.; Li, X.-M. From trace to pure: Recovery of scandium from the waste acid of titanium pigment production by solvent extraction. *Process Saf. Environ. Prot.* **2018**, *121*, 118–124. [CrossRef]
13. Yagmurlu, B.; Orberger, B.; Dittrich, C.; Croisé, G.; Scharfenberg, R.; Balomenos, E.; Panias, D.; Mikeli, E.; Maier, C.; Schneider, R.; et al. Sustainable Supply of Scandium for the EU Industries from Liquid Iron Chloride Based TiO_2 Plants. *Mater. Proc.* **2021**, *5*, 86.
14. Wang, W.; Pranolo, Y.; Cheng, C.Y. Metallurgical processes for scandium recovery from various resources: A review. *Hydrometallurgy* **2011**, *108*, 100–108. [CrossRef]
15. Zhou, G.; Li, Q.; Sun, P.; Guan, W.; Zhang, G.; Cao, Z.; Zeng, L. Removal of impurities from scandium chloride solution using 732-type resin. *J. Rare Earths* **2018**, *36*, 311–316. [CrossRef]
16. Shaoquan, X.; Suqing, L. Review of the extractive metallurgy of scandium in China (1978–1991). *Hydrometallurgy* **1996**, *42*, 337–343. [CrossRef]
17. Van Nguyen, N.; Iizuka, A.; Shibata, E.; Nakamura, T. Study of adsorption behavior of a new synthesized resin containing glycol amic acid group for separation of scandium from aqueous solutions. *Hydrometallurgy* **2016**, *165*, 51–56. [CrossRef]
18. Hérès, X.; Blet, V.; Di Natale, P.; Ouaattou, A.; Mazouz, H.; Dhiba, D.; Cuer, F. Selective Extraction of Rare Earth Elements from Phosphoric Acid by Ion Exchange Resins. *Metals* **2018**, *8*, 682. [CrossRef]
19. Smirnov, A.; Titova, S.; Rychkov, V.; Bunkov, G.; Semenishchev, V.; Kirillov, E.; Poponin, N.; Svirsky, I. Study of scandium and thorium sorption from uranium leach liquors. *J. Radioanal. Nucl. Chem.* **2017**, *312*, 277–283. [CrossRef]
20. Ivanov, N.; Abilmagzhanov, A.; Shokobayev, N.; Adelbayev, I.; Nurtazina, A. Scandium Extraction By Phosphorus-Containing Sorbents. *NAS RK. Ser. Geol. Tech. Sci. Sci. J.* **2020**, *4*, 156–165.
21. Rychkov, V.N.; Nalivayko, K.A.; Titova, S.M.; Abakumova, E.V.; Yakovleva, O.V.; Kirillov, E.V.; Skripchenko, S.Y. Kinetics of scandium sorption from sulfuric acid solutions by ampholyte Lewatit TP260. *AIP Conf. Proc.* **2020**, *2313*, 050028. [CrossRef]
22. Bao, S.; Hawker, W.; Vaughan, J. Scandium Loading on Chelating and Solvent Impregnated Resin from Sulfate Solution. *Solvent Extr. Ion Exch.* **2018**, *36*, 100–113. [CrossRef]
23. Mostajeran, M.; Bondy, J.-M.; Reynier, N.; Cameron, R. Mining value from waste: Scandium and rare earth elements selective recovery from coal fly ash leach solutions. *Miner. Eng.* **2021**, *173*, 107091. [CrossRef]
24. Meshkov, E.Y.; Akimova, I.; Bobyrenko, N.; Solov'ev, A.; Klochkova, N.; Savel'ev, A. Separation of Scandium and Thorium in the Processing of Scandium Rough Concentrate Obtained from Circulating Solutions of In-Situ Leaching of Uranium. *Radiochemistry* **2020**, *62*, 652–657. [CrossRef]
25. Zhu, L.; Liu, Y.; Chen, J.; Liu, W. Extraction of Scandium(III) Using Ionic Liquids Functionalized Solvent Impregnated Resins. *J. Appl. Polym. Sci.* **2011**, *120*, 3284–3290. [CrossRef]
26. Wang, W.; Cheng, C.Y. Separation and purification of scandium by solvent extraction and related technologies: A review. *J. Chem. Technol. Biotechnol.* **2011**, *86*, 1237–1246. [CrossRef]
27. Roosen, J.; Van Roosendael, S.; Borra, C.R.; Van Gerven, T.; Mullens, S.; Binnemans, K. Recovery of scandium from leachates of Greek bauxite residue by adsorption on functionalized chitosan–silica hybrid materials. *Green Chem.* **2016**, *18*, 2005–2013. [CrossRef]

28. Wood, S.A.; Samson, I.M. The aqueous geochemistry of gallium, germanium, indium and scandium. *Ore Geol. Rev.* **2006**, *28*, 57–102. [CrossRef]
29. Reynier, N.; Gagné-Turcotte, R.; Coudert, L.; Costis, S.; Cameron, R.; Blais, J.-F. Bioleaching of Uranium Tailings as Secondary Sources for Rare Earth Elements Production. *Minerals* **2021**, *11*, 302. [CrossRef]
30. Sokolova, Y.V. Sorption of Sc(III) on phosphorus-containing cation exchangers. *Russ. J. Appl. Chem.* **2006**, *79*, 573–578. [CrossRef]
31. Li, Y.; Zhu, Y.; Zhu, Z.; Zhang, X.; Wang, D.; Xie, L. Fixed-Bed Column Adsorption Of Arsenic(V) By Porous Composite Of Magnetite/Hematite/Carbon With Eucalyptus Wood Microstructure. *J. Environ. Eng. Landsc. Manag.* **2018**, *26*, 38–56. [CrossRef]
32. González-López, M.E.; Laureano-Anzaldo, C.M.; Pérez-Fonseca, A.A.; Arellano, M.; Robledo-Ortíz, J.R. A discussion on linear and non-linear forms of Thomas equation for fixed-bed adsorption column modeling. *Rev. Mex. De Ing. Química* **2021**, *20*, 875–884. [CrossRef]
33. Helfferich, F.G. *Ion Exchange*; Courier Corporation: Toronto, Canada, 1995.
34. Han, R.; Wang, Y.; Zou, W.; Wang, Y.; Shi, J. Comparison of linear and nonlinear analysis in estimating the Thomas model parameters for methylene blue adsorption onto natural zeolite in fixed-bed column. *J. Hazard. Mater.* **2007**, *145*, 331–335. [CrossRef]
35. Goel, J.; Kadirvelu, K.; Rajagopal, C.; Kumar Garg, V. Removal of lead(II) by adsorption using treated granular activated carbon: Batch and column studies. *J. Hazard. Mater.* **2005**, *125*, 211–220. [CrossRef]
36. Thomas, H.C. Heterogeneous Ion Exchange in a Flowing System. *J. Am. Chem. Soc.* **1944**, *66*, 1664–1666. [CrossRef]
37. Gallindo, A.D.A.S.; Silva Junior, R.A.D.; Rodrigues, M.G.F.; Ramos, W.B. Modelling and simulation of the ion exchange process for Zn2+(aq) removal using zeolite NaY. *Res. Soc. Dev.* **2021**, *10*, e310101220362. [CrossRef]
38. Lin, L.-C.; Li, J.-K.; Juang, R.-S. Removal of Cu(II) and Ni(II) from aqueous solutions using batch and fixed-bed ion exchange processes. *Desalination* **2008**, *225*, 249–259. [CrossRef]
39. Xiao, Y.; Azaiez, J.; Hill, J.M. Erroneous Application of Pseudo-Second-Order Adsorption Kinetics Model: Ignored Assumptions and Spurious Correlations. *Ind. Eng. Chem. Res.* **2018**, *57*, 2705–2709. [CrossRef]
40. Tran, H.N.; You, S.-J.; Hosseini-Bandegharaei, A.; Chao, H.-P. Mistakes and inconsistencies regarding adsorption of contaminants from aqueous solutions: A critical review. *Water Res.* **2017**, *120*, 88–116. [CrossRef]
41. Weber, T.W.; Chakravorti, R.K. Pore and solid diffusion models for fixed-bed adsorbers. *AIChE J.* **1974**, *20*, 228–238. [CrossRef]
42. Lim, A.P.; Aris, A.Z. Continuous fixed-bed column study and adsorption modeling: Removal of cadmium (II) and lead (II) ions in aqueous solution by dead calcareous skeletons. *Biochem. Eng. J.* **2014**, *87*, 50–61. [CrossRef]
43. Fallah, N.; Taghizadeh, M. Continuous fixed-bed adsorption of Mo(VI) from aqueous solutions by Mo(VI)-IIP: Breakthrough curves analysis and mathematical modeling. *J. Environ. Chem. Eng.* **2020**, *8*, 104079. [CrossRef]
44. Wang, W.; Pranolo, Y.; Cheng, C.Y. Recovery of scandium from synthetic red mud leach solutions by solvent extraction with D2EHPA. *Sep. Purif. Technol.* **2013**, *108*, 96–102. [CrossRef]